ARISTOTELIO UNIVERSITY OF THESSALONIKI Polytechnic School
Department of Mechanical Engineering
MECHANICAL DYNAMICS Laboratory

STRUCTURAL DYNAMICS

FIXED WING STRUCTURAL MODELING AND ANALYSIS

Author : Diogenis Tsichlakis

Modeling and analysis of the lower left wing of a Skybolt airplane by Steen Aero Lab Inc. In Figure 1. the plane on which the wing under study is marked is depicted. In Figure 2. the modeled form of the lower left wing of the airplane is shown. Also in Figure 2, Detail A is noted, which is one of the wing's 11 airfoils. Detail A is shown enlarged in Figure 3, in which characteristic dimensions of the airfoil are already noted.

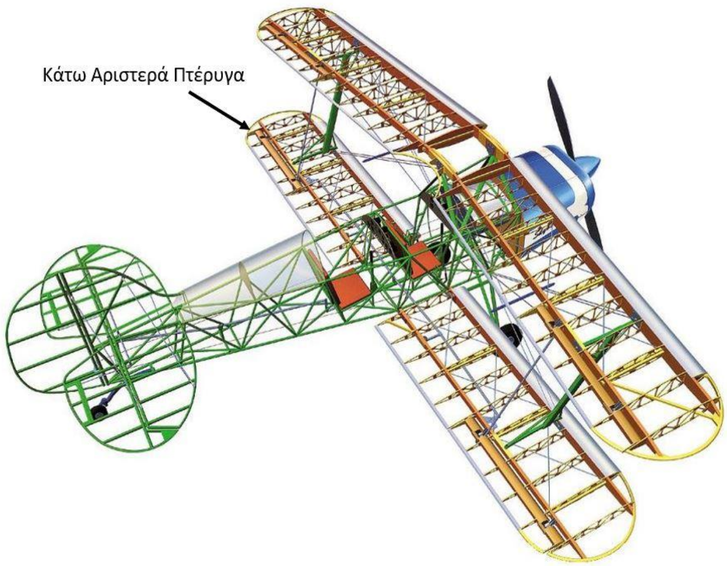

Figure 1. Skybolt airplane, by Steen Aero Lab Inc

Observing Figure 2. we distinguish 2 different colorings for modeling the wing. Red elements symbolize bar elements and blue elements beam elements. In addition, the blue elements that join the airfoils are also beam elements. In Figure 2. you can also see the distance d, between 2 airfoils and Detail A. which includes the airfoil you represent in Figure 3.

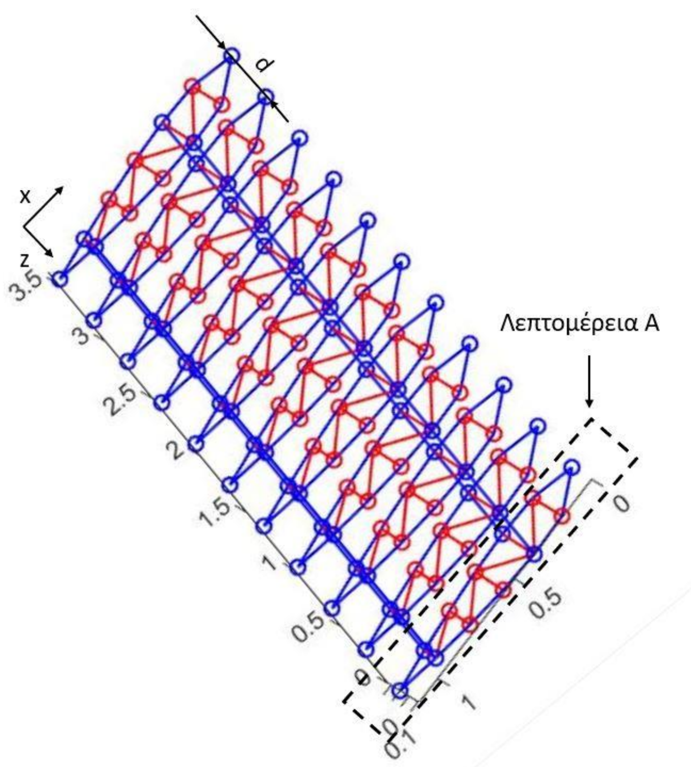

Figure 2. Wing visualization with bar and beam elements, using Matlaab software

Figure 3 shows one of the 11 airfoils on our wing. Also marked on the airfoil are the characteristic sizes of the chord length. Airfoil NACA 2116 (which is parametrized and can be changed). For the modeling we use per airfoil 12 nodes, 12 flexural elements around the airfoil and 9 axial elements inside. Also in total on the wing there are also (11-1) elements of beams through which the airfoils are joined. Therefore our model consists of a total of 12*11=132 nodes, 11*9=99 axial elements and 12*11+4(11-1)=172 beams.

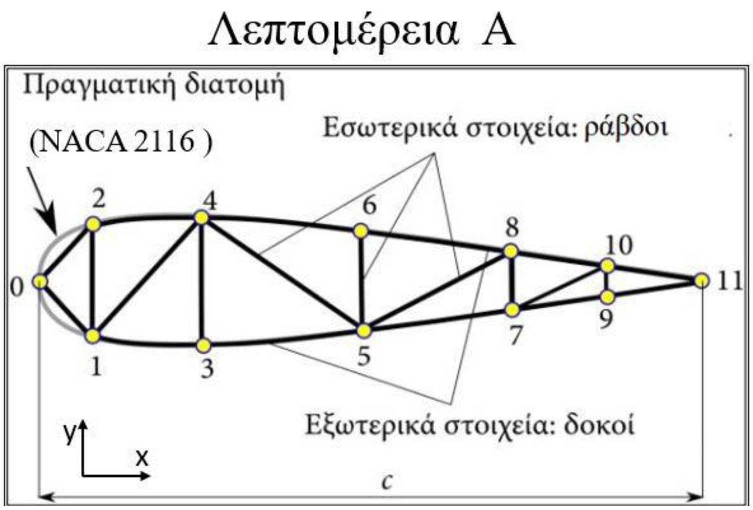

Figure 3. Detail A, NACA 2116 airfoil

In Table 1. the geometrical dimensions are summarized. In addition, in Table 1. are also the basic geometric quantities calculated using the data.

Table 1. Data and Characteristic sizes

Aerofoil	NACA 2116	Loading Fo	500 N
String length c	1.12 [m]	Cross section of elements A	0.0031 m^2
Wing Length L	3.61 [m]	Density p	2700 $\frac{kg}{m^3}$
Cross-sectional radius r	0.0316 [m]	Surface Moment of Inertia I	7.8314 10^{-7}
Modulus of elasticity E	69 [GPa]	Pole moment of inertia J	7.8314 10^{-7}
Poisson's ratio n	0.35	Shear measure G	25.5 [GPa]
Spacing of airfoils d	0.36 [m]		

The distance of the airfoils:$d = \frac{Wing\ Length(L)}{Airfoil\ Number-1}\quad [m]$

In the table above, the cross-section of elements was calculated:$A = \pi\, r^2\quad [m^2]$

The surface moment of inertia : , which is equal to the polar J for circular solid cross-section of beam and rod elements.$I = \frac{\pi\, r^4}{4}\quad [m^4]$

The shear modulus:$G = \frac{E}{2(\nu+1)}\quad [GPa]$

Density was obtained from Tables for aluminum which is our material in , also for calculations lengths are kept in meters, forces in Newton and material properties E,G in Pascal (.$[\frac{\mathrm{kg}}{m^3}]1GPa = 10^9 Pa$)

The airfoil's coordinates are taken from:http://airfoiltools.com/airfoil/naca4digit**.**

All the Graphs, equations and analysis can be found in the structural dynamics code written in Python, following Object-Oriented Programming principles.

The requested :

This Report includes the following:

> **A) The six lowest and six highest eigenfrequencies and eigenmodes of the wing in question.**
> **B) The static response at node 12z for static loading F=F0.**
> **C) The frequency-response diagram at node 12z for harmonic loading F(t)=F0 sin(Ωt), for 0 < Ω < ω6.**
> **D) The response at node 12z for harmonic loading F(t)=F0 sin(Ωt), with Ω=ω2. To compare the solution with the eigenform analysis method and the Newmark method (with α=0.25 and β=0.50).**

In the last two questions, choose Rayleigh type damping which leads to a damping measure of 0.01 in the first singular form and 0.02 in the sixth singular form.1422

PROBLEM A

To calculate the eigenfrequencies and eigenforms with the finite element method, the following steps are generally performed:

- Data Tables are created: Nodes, Elements, Forces, Boundary Conditions, Material Properties.
- Calculation of Local stiffness and mass matrices for each element
- Calculation of Matrices of Coordinate Transformations (Rotational Freedoms)
- Calculation of localization vectors (matching local-general degrees of freedom)
- Calculation of total Matrices of robustness, mass and force vector
- Solving differential equations with the method of eigenform analysis
- Finding Eigenfrequencies and Eigenmodes

The following figures depict the first six elastic eigenmodes of our wing and the eigenfrequencies respectively.

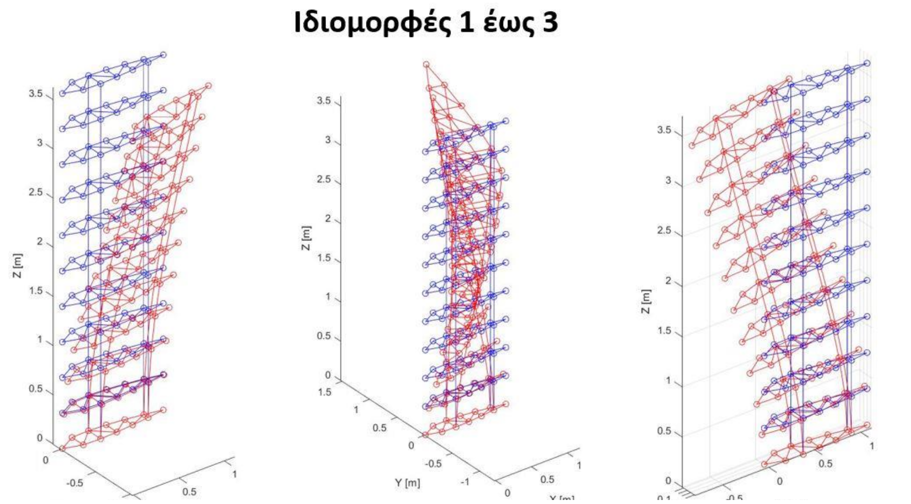

Figure 4. The first 3 singularities of the wing and the corresponding eigenfrequencies of each singularity. Visualization was performed with Python software

Figure 5. Eigenmodes 4 to 6, of the wing and the corresponding eigenfrequencies of each eigenmode

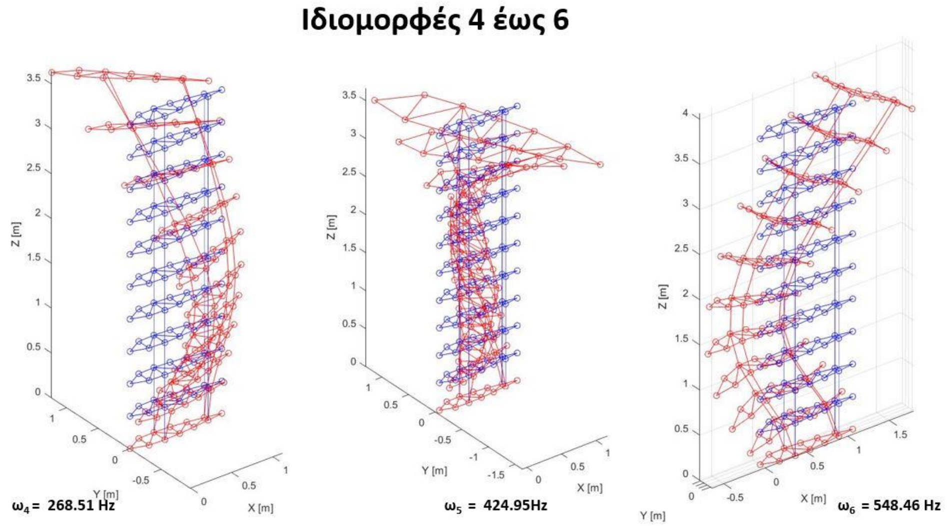

In the 4 Figures, the unloaded state of the wing is depicted in blue and the deformed state of the wing in red for each eigenfrequency.

Observing the 4 figures we see that the displacements are stronger in the 6 lowest eigenfrequencies than in the 6 highest ones. This fact can be due to 2 situations. First, because in the last singularities, the natural frequencies are so high (about 5 orders of magnitude higher), the wing does not have time due to inertia to follow the oscillation and thus the oscillation ranges are from small to negligible. Secondly, the characteristics of the wing (solidity and mass) are such that for such high excitation frequencies we maintain smaller oscillation ranges. Finally we see that the 1st airfoil for all eigenfrequencies remains unchanged, as we expected since this airfoil includes the 4 clamped nodes.

We can still distinguish that the 1st and 3rd singularities are purely flexural with respect to the X and Y axes respectively, while the 2nd torsional singularity. Unlike 4 to 6 which are a combination of bending and torsion.

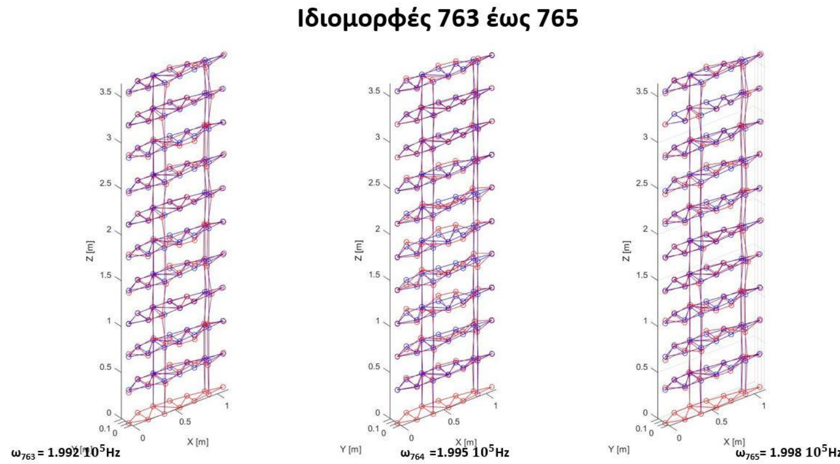

Figure 6. Eigenmodes 763 to 765, of the wing and the corresponding eigenfrequencies of each eigenmode.

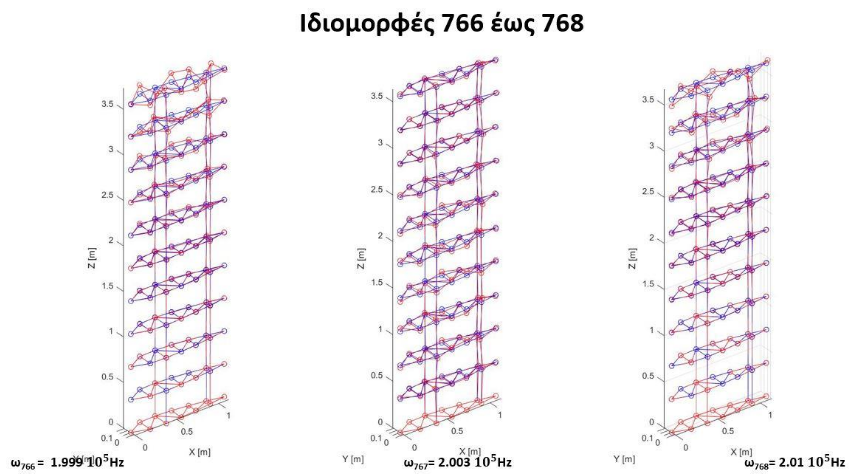

Figure 7. Eigenmodes 766 to 768, of the wing and the corresponding eigenfrequencies of each eigenmode.

When visualizing idiotypes we are essentially depicting in 3D diagrams displacements and rotations of nodes and not the deformations along the elements. To satisfy the latter we would have to return the calculated degrees of freedom in the local coordinate systems and then the perturbation functions of each element should be used. Thus we would end up with a more realistic representation of the singularity for the wing.

PROBLEM B

The static solution is calculated from: v_static = K\F

This is how the static displacements of the nodes are calculated. First, the static response is visualized for all nodes of the wing, Figure 8. In this figure, the initial condition of the wing at no load is depicted in blue and in red the response of the wing for the static load Fo. To make the static responses clearly visible, we enlarged them by multiplying them by a factor of scale=100.

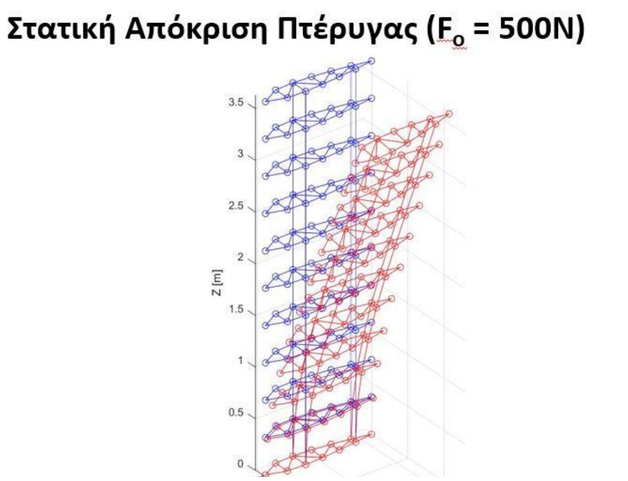

Figure 8. Static Wing Response for loading in the y direction, Fo = 500 N

To find the response of node 126(for me z=6) as you ask, we look at the v_static vector. This vector contains 768 elements, which are the total degrees of freedom of the wing minus the freedoms we contracted. Therefore to find the positions where the displacements of freedom of node 126 are located we work as follows. Each airfoil has 12 nodes so node 126 is a node of the last airfoil. The only fixed nodes on the wing are 4 and are those of the 1st airfoil, with 6 degrees of freedom each. Thus, between the node we are interested in and the 1st node, 4 nodes have been removed (their degrees of freedom). Therefore we have that the degrees of freedom for our node start from the position: (12z-1) x 6 +1-(Fixed nodes) =727 for z=6.

Table 2, has the values for the 6 dofs of node 72.

Table 2 . Node 72 static response

x	$-12\ 10^{-5}\quad [m]$	thx	0.004 [˚]
y	-0.0118 [m]	thy	$-9.3\ 10^{-5}$[˚]

z	$-22.9\ 10^{-5}\ [m]$	thz	0.00149 [˚]

We see that the maximum displacement, as expected, occurs in the y direction of the load Fo, as we can also see in Figure 8. Accordingly, the turn in y is the smallest of the 3rd. This behavior is due to the fact that our load has a direction to Y, therefore with a DES (Free Body Diagram) we could see that the Load creates a bend with respect to X. where and observing Table 2. we have the maximum turn at the node us. We also know that node 126, looking at Figure3. located approximately in the middle of the last airfoil. A node in a more extreme position than 126 for the same airfoil would give about the same turn for Y and X, but more for Z. These conclusions are easily obtained by observing the above Figure.

QUESTION C

In the last 2 questions of our paper, you ask for Rayleigh type damping to be chosen which leads to a damping measure of 0.01 in the 1st singularity and 0.02 in the 6th singularity.

We know that the Rayleigh damping register is calculated from the equation:

$C = aM + \beta K$

where M,K are the total matrices of our wing and additionally α,β are scalar constants. By applying the Caughey method and simultaneously applying the orthogonality conditions (verticality of the eigenforms) for the 1st and 6th eigenfrequency, the following system of equations is obtained:

$$\begin{cases} 2\zeta_1\omega_1 = \alpha + \beta\omega_1^2 \\ 2\zeta_6\omega_6 = \alpha + \beta\omega_6^2 \end{cases}$$

Having calculated in the previous questions the first 6 eigenfrequencies of the wing, we can calculate by solving the system the constants α,β specifically for ω1 = 51.8508 Hz and ω6 = 548.4605 Hz we have:

α = 0.8485, β = 0.0001

In the 3rd question you ask for the response frequency diagram at node 12z = 126 for harmonic loading of the form F= Fo sin(Ωt), for excitation frequency 0< Ω <ω6 . So you ask for the plot of the range of the response for different excitation frequencies. Our response is of the form:

$$w_e(x,y,z,t) = \sum_{n=1}^{n_e} \Phi_{n_e}(x_e,y_e,z_e)v_e(t)$$

$where v_e(t)$the time responses of the degrees of freedom of each element At its nodes,$n_e$the number of shape functions for each element (beam or bar) and the shape functions of each element. Since we are interested in the frequency response at a node and since the shape functions at the nodes are chosen to take a value of 0 or 1, it suffices to calculate the time coefficients$\Phi_{n_e}(x_e,y_e,z_e)v_e(t)$.

Having calculated the total matrices of the wing, we arrive at the quadratic differential equation:

$$M\ddot{v} + C\dot{v} + Kv = F(t)$$

which is written in the form:

$$M\ddot{v} + C\dot{v} + Kv = f_s \sin(\Omega t) + f_c \cos(\Omega t)\,, \qquad \mu\varepsilon \;\; f_c \; = 0_{Nx3}$$

Where the matrices M,C,K are the total matrices of the structure, the excitation register is also the total register for the wing and the vector v is the vector of the displacements at the nodes of the whole wing as a function of time, having of course, as mentioned above, removed the contracted liberties. All matrices mentioned have been calculated in the preceding analysis.f_s

We now know from the oscillations that for harmonic loading as we have and here we can assume that in the steady state our solution will be of the form: $v(t) = \; v_s \sin(\Omega t) + v_c \cos{(\Omega t)}$

by substituting this solution in the above differential we end up with a system of 2N x 2N equations (N= total number of wing freedoms) the solution of which will give us the time responses we are looking for, for a selected Ω. The system we end up with is the following:

$$\begin{bmatrix} K - \Omega^2 M & \Omega C \\ \Omega C & \Omega^2 M - K \end{bmatrix} \begin{bmatrix} v_c \\ v_s \end{bmatrix} = \begin{bmatrix} 0_{Nx3} \\ -f_s \end{bmatrix}$$

The calculation of the vector and , is carried out with the code shown on the right. Having now calculated the desired vectors, we replace them in the expression$v_s v_c v(t) = \; v_s \sin(\Omega t) + v_c \cos{(\Omega t)}$

The calculation is done using an iterative process with the excitation frequency running in the previously defined range.

To be able to make the graph, we must have a trigonometric in our final relationship, so that we can then work with the ranges of the vector v(t) for each Ω and neglect the time dependence of the trigonometric. We use the basic trigonometric equation

$$\mathrm{Acos(x)} - \mathrm{Bsin(x)} = \mathrm{Rcos(c} + \theta)$$

where for our example:

$$R = \sqrt{{v_c}^2 + (-v_s)^2}$$

$$\theta = \tan^{-1} \frac{-v_s}{v_c}$$

So we end up with the time response of the nodes:$v(t) = \; Rcos(\Omega t + \theta)$

Thus we obtain the desired frequency response diagram from the representation of the equation R=R(Ω) for the freedoms of interest (727:732).

In case we wanted the same diagram for a point e.g. in the middle of some element we should transfer the displacements to the nodes of the element in the local coordinate system and then through the interpolation functions (depending on the type of element) get the requested diagram.

Finding the positions we are interested in for node 126 is done as in query B((12z-1+(Fixed nodes)) x 6 +1 =727 to 729) . We in Figures 9 to 11 visualize the displacements in the x,y,z directions for Ω from 0 to ω6 with a step of 0.5.

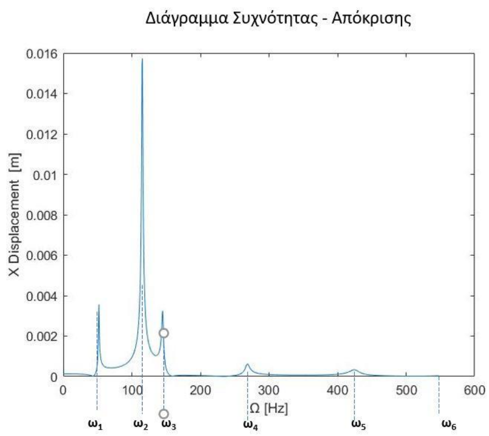

Figure 9. Frequency-Response Diagram of node 126, in the X direction for Ω= 0 to 548.46 Hz

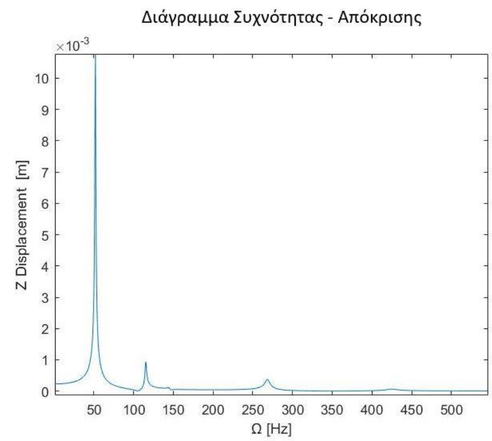

Figure 10. Frequency-Response Diagram of node 126, in the Z direction for Ω= 0 to 548.46 Hz

Looking at Figures 9 and 10, we see the frequency response plots for node 126 in the X,Z directions. On the vertical axis, we see that the displacement measures are small especially in the z direction, along the wing. Also as expected we distinguish multiple resonances for excitation frequencies equal to the eigenfrequencies of the wing. In the diagram of X we see 5 resonances while in Z, 3. This fact is due to the stimulation of the construction, because as we know, a stimulation is not necessary to stimulate all the singularities of our construction in all directions.

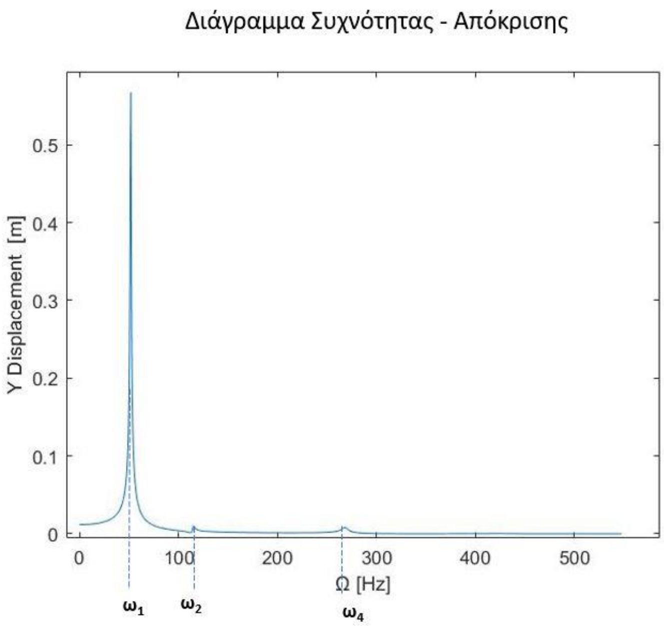

Figure 11. Frequency-Response Diagram of node 126, in the Y direction for Ω= 0 to 548.46 Hz

In Figure 11. we see the frequency response in the Y direction, where we notice that there also appear the largest oscillation ranges during the resonances. This behavior is logical since the charge vector is in this direction. As before we observe 3 resonances instead of the 6 that one would expect due to the existence of 6 eigenfrequencies in this interval. You explain this as before, due to the charging of some singular form by some stimulation. A particularly high range of oscillation is given by the resonance at the 1st eigenfrequency for the y-freedom. In the above diagrams, the eigenfrequencies corresponding to each resonance are also noted.

The results we distinguished in the last Figure for the shift in Y, can also be verified by the analysis we did for the 1st question of the paper. Referring to Figures 4 and 5. we can see for the 1st 6 eigenmodes the maximum displacement in the Y axis appears for the 1st eigenmode (1st eigenfrequency) that we have a clear bending as we also saw in the diagram of Figure 11 that for the 1st eigenfrequency we have resonance and even in the maximum range. We also see that the eigenfrequency 2 which corresponds to the almost perfectly torsional eigenmode 2, causes a minimal increase in amplitude. Whereas for $\Omega=\omega 3$ where we have a pure bending with respect to Y, we see that the freedom in Y of node 126 is not excited at all.

With a corresponding logic, we can also relate the behavior we see in Figure 11. for the remaining eigenfrequencies, with Figures 4 and 5 of the eigenforms or with figures 9 and 10 for the other 2 directions (X,Z). So we confirm the results for the resulting frequency response plots.

PROBLEM D

In the 4th question, you ask to calculate the response of node 12z=126 for harmonic loading F= Fo sin(Ωt) with Ω=ω2=115.2838 Hz, initially with the eigenform analysis method and then with the Newmark method and to compare them for the its overall condition (transitional and permanent).

IMPLEMENTATION OF EIGENMODE ANALYSIS

By means of the finite element method we have arrived at the total robustness, mass and excitation matrices. We have also calculated the damping register C, for Rayleigh type damping. Thus we arrived at a coupled system of linear differential equations of the form:

$$M\ddot{v} + C\dot{v} + Kv = F(t) \quad (\mathbf{1})$$

where are the time functions of the displacements for the nodes of the wing.$\mathrm{v} = \mathrm{v(t)}$

The solution for the response of the nodes as a function of time (you consist of 2 terms, you consist of the partial solution that refers to the steady state and depends on the excitation and the homogeneous solution that you refer to the transient state and depends on the characteristics of the oscillator (wing) whose effect is amortized after a certain period of time. The system (1) is a system of linear differential equations and in order to be able to be solved it requires a transformation of its coordinates so that its functions are disentangled and can be solved as single-degree linear oscillators.$v(t)$)

Before we proceed to find the answer we need to narrow down the area of our analysis and exclude pieces of less importance.

We know that singularities with eigenfrequencies in the range :

$$\omega_i < \frac{\Omega}{3}(\ 38.428\ Hz) \quad ή \qquad \omega_i > 3\Omega\ (345.85\ Hz)$$

they do not significantly affect the dynamic response of our system, so they can be neglected. This is easily understood if we consider the diagram for the open displacement range (X) and the open excitation frequency (η=Ω/ω) of a single stage oscillator. Observing this diagram, we see that when we are in the 1st case then X→1 so we tend to the static response, while when we are in the 2nd case then X→0 so our answer is very small.

Solution for System(1)

$$M\ddot{v} + C\dot{v} + Kv = F(t)$$

the

$$M\ddot{v} + C\dot{v} + Kv = f_s \sin(\Omega t) \quad (\mathbf{2})$$

Initially by applying the eigenmode analysis we remove the damping and the excitation and solve the eigenproblem from where and by solving the determinant we find the eigenfrequencies first and then the corresponding eigenmodes.$(K - \omega^2 M)\widehat{x_i} = 0$

The procedure described has been done in Question B. From the eigenforms we calculated, we keep those that have eigenfrequencies in the value range . Specifically, for our own problem, within the code, the eigenfrequencies that are within the limits are found. Therefore, only the first 4 eigenfrequencies of the wing will participate in the analysis, because the eigenfrequencies of the rest are out of bounds.$\omega_i \in (38.428, 345.85)$

Then, having preserved the singularities that interest us, we create the table of singularities, with columns of the singularities of the system. The singularities as known form a base of the space since they are perpendicular to each other. Since the system (1) is entangled, we need a transformation to be able to disentangle the equations from each other, by means of the transfer to another coordinate system. We know from the orthogonality conditions for singularities that:$\Phi_{NxN'}$

$$\Phi^T M \Phi = I$$

$$\Phi^T K \Phi = \Lambda$$

$$\Phi^T C \Phi = Z$$

where the matrices are diagonal. Therefore we will arrive at decoupled equations using the transformation.I, Λ, Z

Thus means of transformation$v(t) = \Phi\tau(t) \ \Rightarrow \tau(t) = \ \Phi^T M v(t)$ $(\mathbf{3})$

where the dimensions$v = v_{Nx1} \ \ , \ \ \tau = \tau_{N'x1}$

and transfers our responses from the original coordinates v(t) to the new(main) coordinates τ(t). Where N, the total degrees of freedom of our wing and N', the number of eigenforms we keep to describe our solution (which is in the range of eigenfrequencies we defined earlier).

Returning to system (2), we substitute the transformation (3) and multiply all terms from the left by the inverse of the eigenform matrix.

$$\Phi^T M\Phi\ddot{\tau} + \Phi^T C\Phi\dot{\tau} + \Phi^T K\Phi\tau = \Phi^T f_s \sin(\Omega t)$$

$$\Rightarrow \qquad \widehat{M}\ddot{\tau} + \hat{Z}\dot{\tau} + \hat{\Lambda}\tau = p(t)$$

where $\Phi^T M_{NxN}\Phi = I_{N'xN'}$

with $\Phi^T C_{NxN}\Phi = Z_{N'xN'}Z = \begin{pmatrix} 2\zeta_1\omega_1 & \cdots & 0 \\ \vdots & \ddots & \vdots \\ 0 & \cdots & 2\zeta_i\omega_i \end{pmatrix}$

with$\Phi^T K_{NxN}\Phi = \Lambda_{N'xN'}\Lambda = \begin{pmatrix} \omega_1^2 & \cdots & 0 \\ \vdots & \ddots & \vdots \\ 0 & \cdots & \omega_i^2 \end{pmatrix}$

$\Phi^T F_{Nx1} = p_{N'x\,1} = \hat{p}\sin\,(\Omega t)$

Finally we arrive at a system of decoupled linear differential equations in terms of the principal coordinates τ(t) and εsolve the single-stage oscillator equation:

for the i singularity (i=1 to N'=4)$\ddot{\tau_\iota} + 2\zeta_i\omega_i\dot{\tau_\iota} + \omega_i^2\tau_i = \; \widehat{p_\iota}\sin\,(\Omega t)$ $\;(\mathbf{4})$

The solution of the differential equation (4) consists of 2 terms, the homogeneous and the inhomogeneous. As we analyzed before the 1st refers to the characteristics of the oscillator and decays after a point, while the 2nd refers to the characteristics of the excitation.

<u>Homogeneous Solution</u>

To solve the homogeneous problem we subtract the excitation from Eq. (4) :

$$\ddot{\tau_\iota} + 2\zeta_i\omega_i\dot{\tau_\iota} + \omega_i^2\tau_i = 0 \;\; (\mathbf{5})$$

Because the motion equation (5) is linear and has constant coefficients, it has solutions of the form:

$$\tau_i = ae^{\lambda t}$$

substituting the solution in (5) gives us:

$$(\lambda^2 + 2\zeta_i\omega_i\lambda + \omega_i^2)\alpha e^{\lambda t} = 0$$

Solving the 2nd degree polynomial in the parenthesis we get:

$$\lambda_{1,2} = -\zeta_i\omega_i \pm i\omega_{di}$$

$with\omega_{di} = \omega_i\sqrt{1-\zeta_i^2}$

Thus the initial solution along with Euler's identity:

$(e^{\pm i\omega_{di}t} = \cos(\omega_{di}t) \pm isin(\omega_{di}t))$

comes in the form:

$$\tau_i(t) = e^{-\zeta_i\omega_i t}[A_i \cos(\omega_{di}t) + B_i \sin(\omega_{di}t)] \quad (\mathbf{6})$$

Where the constants Ai,Bi are calculated at the end by applying the initial conditions.

Partial solution

In searching for the partial solution you ask us to solve the system:

$$\ddot{\tau} + Z\dot{\tau} + \Lambda\tau = \hat{p}\sin(\Omega t) + \widehat{p_o}\cos(\Omega t) \ ,\mu\varepsilon\ \widehat{p_o} = 0 \quad (\mathbf{7})$$

We know that for harmonic excitation in oscillators one degree of freedom in the steady state (partial solution) is of the form:

$$\tau_\mu(t) = \tau_s \sin(\Omega t) + \tau_c \cos(\Omega t) \quad (\mathbf{8})$$

Where by substitution in the non-homogeneous system (7), we equate the trigonometric coefficients and solve in terms of τs, τc , we end up with the system:

$$\begin{bmatrix} \Lambda - I\Omega^2 & \Omega Z \\ \Omega Z & \Omega^2 I - \Lambda \end{bmatrix} \begin{bmatrix} \tau_c \\ \tau_s \end{bmatrix} = \begin{bmatrix} 0_{Nx3} \\ -\hat{p} \end{bmatrix}$$

Solving this system as in Γ gives us the partial solution for Ω=ω2 as a function of time.

Finally, the time response of the nodes in terms of the main coordinates results from the superposition of a partial and homogeneous solution:

$$\xRightarrow{(6),(8)} \tau(t) = \tau_{o\mu o}(t) + \tau_\mu(t)$$

$$\tau_i(t) = e^{-\zeta_i\omega_i t}[A_i \cos(\omega_{di}t) + B_i \sin(\omega_{di}t)] + \tau_{si}\sin(\Omega t) + \tau_{ci}\cos(\Omega t) \quad (\mathbf{9})$$

Now having the total response in terms of , we derive equation (9) in terms of time and have:τ_i

$$\begin{aligned} \dot{\tau}_i(t) = -\zeta_i\omega_i e^{-\zeta_i\omega_i t}[A_i \cos(\omega_{di}t) + B_i \sin(\omega_{di}t)] \\ + e^{-\zeta_i\omega_i t}[-\omega_{di}A_i \sin(\omega_{di}t) + \omega_{di}B_i cos(\omega_{di}t)] + \Omega\tau_{si} cos(\Omega t) \\ - \Omega\tau_{ci}\sin(\Omega t) \quad (\mathbf{10}) \end{aligned}$$

For zero initial conditions, application of the transformation (3) gives:$v(0)\dot{v}(0)$

$$\tau(0) = \Phi^T M v(0) = \begin{bmatrix} 0 \\ 0 \\ 0 \\ 0 \end{bmatrix}$$

$$\dot{\tau}(0) = \Phi^T M \dot{v}(0) = \begin{bmatrix} 0 \\ 0 \\ 0 \\ 0 \end{bmatrix}$$

Substitution in (9),(10) Give :

$$\begin{cases} 0 = A_i + \tau_{ci} \\ 0 = -\zeta_i \omega_i [A_i] + [\omega_{di} B_i] + \Omega \tau_{si} \end{cases}$$

$$\Rightarrow \begin{cases} A_i = -\tau_{ci} \\ B_i = \dfrac{-\zeta_i \omega_i [\tau_{ci}] - \Omega \tau_{si}}{\omega_{di}} \end{cases} \quad \mathbf{(11)}$$

Finally by substituting solutions (11), in (9) we have for the main coordinates:

$$\tau_i(t) = e^{-\zeta_i \omega_i t} \left[-\tau_{ci} \cos(\omega_{di} t) + \left(\frac{-\zeta_i \omega_i [\tau_{ci}] - \Omega \tau_{si}}{\omega_{di}}\right) \sin(\omega_{di} t) \right] + \tau_{si} \sin(\Omega t) + \tau_{ci} \cos(\Omega t) \quad \mathbf{(12)}$$

Now the transformation (3) is used again to return to the original coordinates: $v(t) = \Phi \tau(t)$

NEWMARK METHOD AND COMPARISON

The Newmark method is a numerical integration method.

In Figures 12 and 13, the responses given by the 2 methods in the X direction are presented, while in Figures 14 and 15 in the Y direction.

Representation of the responses was performed for a duration of 5 seconds and an integration time step of 0.0005 for the Y direction. For the X direction we keep the same features but reduce the final completion time to 1 second so that the similarity of the methods is more noticeable.

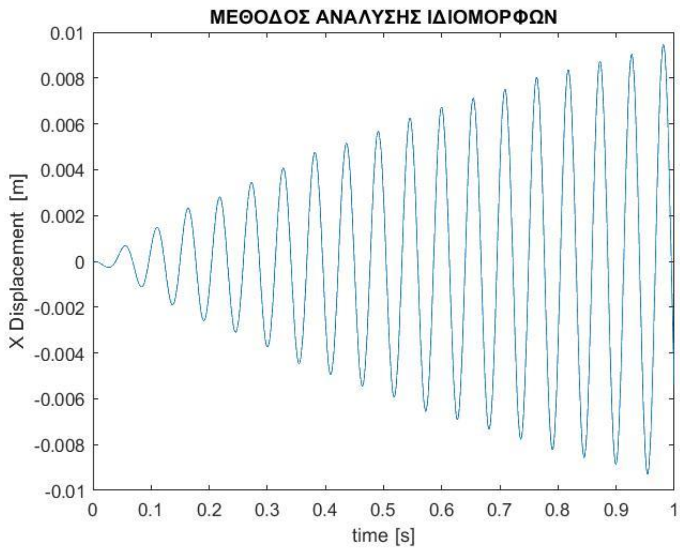

Figure 12. Oscillatory response of node 126, in the X direction with the eigenform analysis method

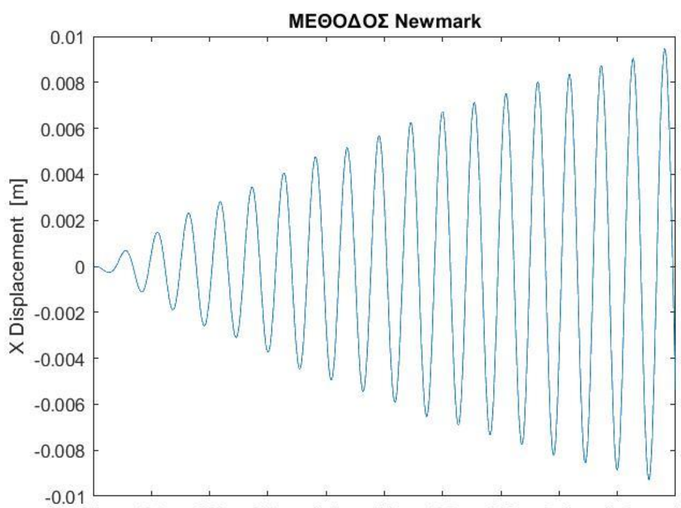

Figure 13. Oscillatory response of node 126, in the X direction with the Newmark method

Figures 12 and 13 are used to verify the identity of the 2 methods. Observing these Figures we can see that the α results are completely identical between the 2 methods.

We also distinguish the increasing trend of the amplitude of the oscillation. This range continues to increase until the effect of the homogeneous solution is extinguished and only the effect of the excitation prevails (steady state), where we will now have arrived at a stable harmonic oscillation.

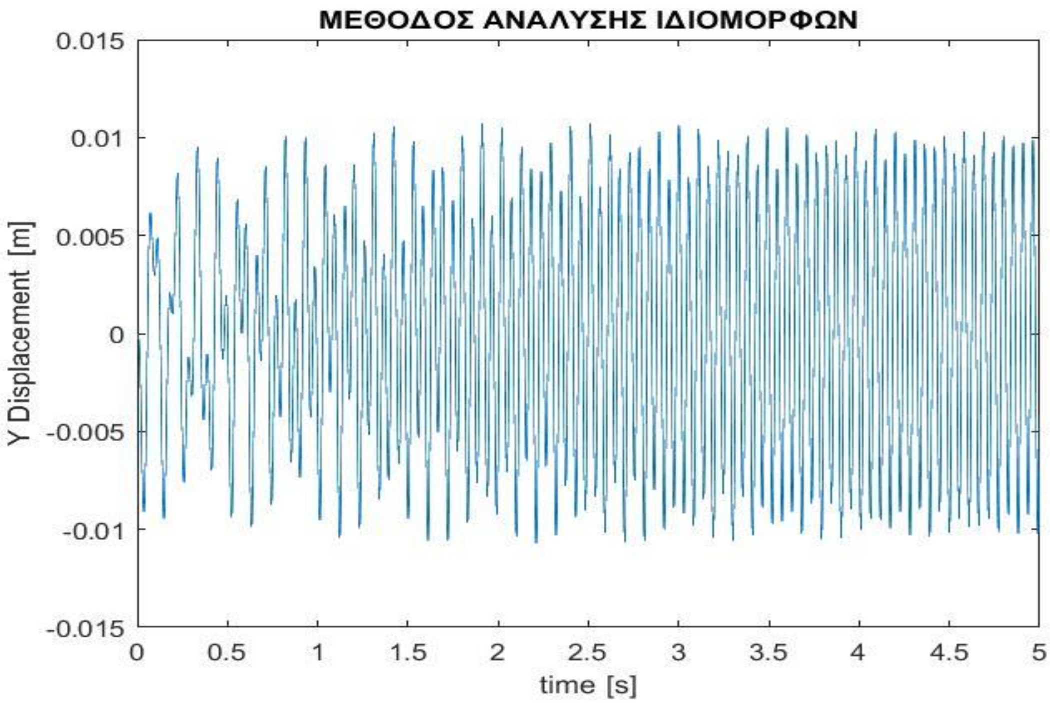

Figure 14. Oscillatory response of node 126, in the Y direction with the eigenform analysis method

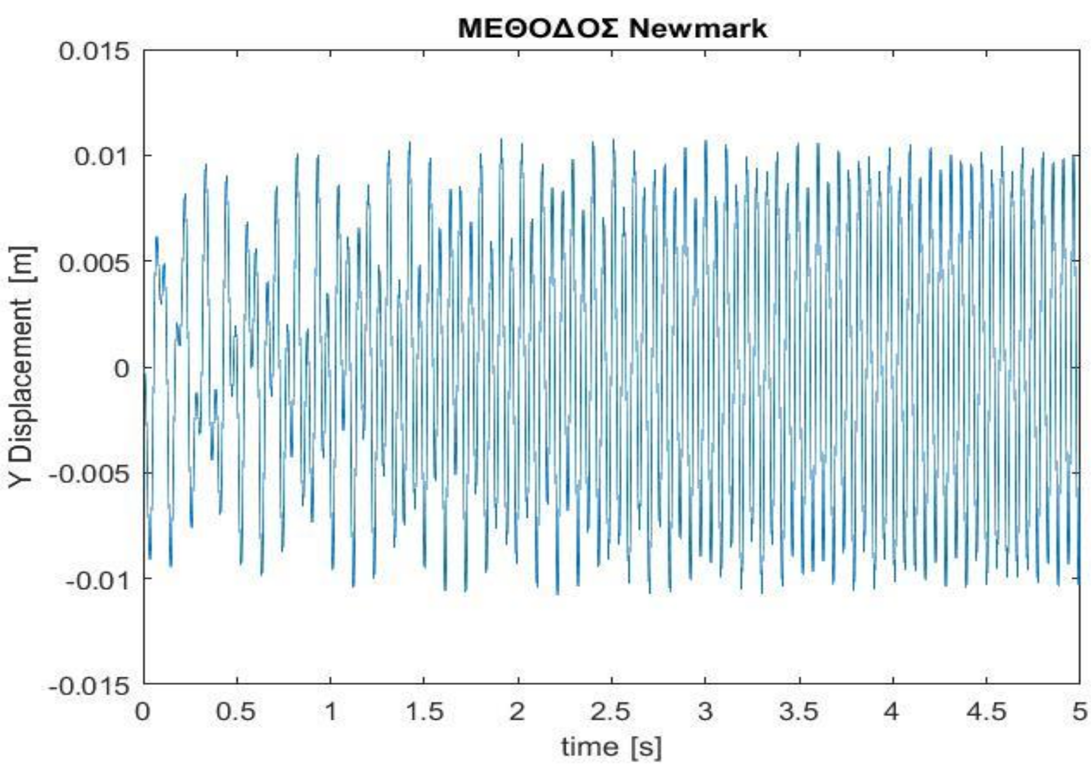

Figure 15. Oscillatory response of node 126, in the Y direction with the Newmark method

From Figures 14 and 15, for the Y direction, we first see that the 2 methods give us the same answers. This confirms the functionality of our code. We see that initially the effect on the characteristics of the oscillator (transitional state) is stronger than the excitation. After some time, of course, the excitation prevails and the oscillatory behavior of node 126 ends up in the permanent state where you stabilize its behavior. In addition, we can see that the amplitude of the oscillation in the steady state exhibits periodic fluctuations. These fluctuations are called fluctuations. This behavior is due to the fact that during the analysis and solution of the linear differential equations of the decoupled system, harmonic terms with equal frequencies are added. Because in the permanent state the condition that remains and prevails is:

$$\tau_i = \tau_{si} \sin(\Omega t) + \tau_{ci} \cos(\Omega t)$$

This behavior indicates the periodic transfer of energy between the nodes of the system, in such a way that the total energy of each singularity remains constant. One could also see a periodic behavior weaker of course for the transition state as well. In general, detonations occur in the transient state for small damping measures.

Still observing the vertical axis in the diagrams of the 2 different directions, as we also saw in question B, the range of oscillation in the Y direction is greater than X, as we also observed for the range of resonance in the 2nd natural frequency for these 2 directions. This behavior was expected if we consider the loading direction of our structure.

Finally, Figures 16 and 17 show the responses of the degrees of freedom θX , θY for node 126.

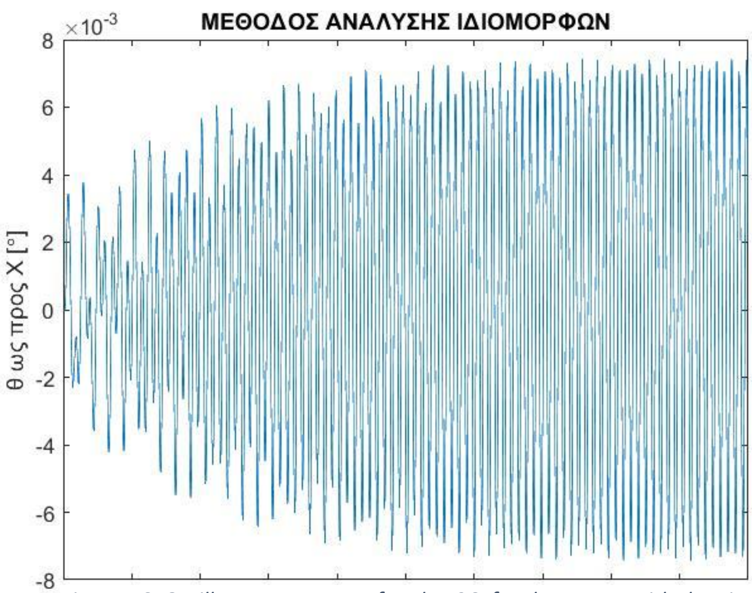

Figure 16. Oscillatory response of node 126, for the Y turn, with the eigenform analysis method

We notice in the Figures that the behavior of the 2 degrees of freedom in the steady state have been reversed in terms of directions. Now for the turns I have crashes in the steady state more strongly in the X time while for the Y we are led to a more stable steady state with less pronounced abovephenomenon. In addition we distinguish that the oscillation ranges of freedom θXare bigger than the other. This is due to the creation of a greater bending load on X than on Y.

Figure 17. Oscillatory response of node 126, for turning in X, with the eigenform analysis method